

UC Irvine

UC Irvine Previously Published Works

Title

Neuroanatomical heterogeneity and homogeneity in individuals at clinical high risk for psychosis

Permalink

<https://escholarship.org/uc/item/1m2044hm>

Journal

Translational Psychiatry, 12(1)

ISSN

2158-3188

Authors

Baldwin, Helen
Radua, Joaquim
Antoniades, Mathilde
[et al.](#)

Publication Date

2022

DOI

10.1038/s41398-022-02057-y

Copyright Information

This work is made available under the terms of a Creative Commons Attribution License, available at <https://creativecommons.org/licenses/by/4.0/>

Peer reviewed

ARTICLE OPEN



Neuroanatomical heterogeneity and homogeneity in individuals at clinical high risk for psychosis

© The Author(s) 2022

Individuals at Clinical High Risk for Psychosis (CHR-P) demonstrate heterogeneity in clinical profiles and outcome features. However, the extent of neuroanatomical heterogeneity in the CHR-P state is largely undetermined. We aimed to quantify the neuroanatomical heterogeneity in structural magnetic resonance imaging measures of cortical surface area (SA), cortical thickness (CT), subcortical volume (SV), and intracranial volume (ICV) in CHR-P individuals compared with healthy controls (HC), and in relation to subsequent transition to a first episode of psychosis. The ENIGMA CHR-P consortium applied a harmonised analysis to neuroimaging data across 29 international sites, including 1579 CHR-P individuals and 1243 HC, offering the largest pooled CHR-P neuroimaging dataset to date. Regional heterogeneity was indexed with the Variability Ratio (VR) and Coefficient of Variation (CV) ratio applied at the group level. Personalised estimates of heterogeneity of SA, CT and SV brain profiles were indexed with the novel Person-Based Similarity Index (PBSI), with two complementary applications. First, to assess the extent of within-diagnosis similarity or divergence of neuroanatomical profiles between individuals. Second, using a normative modelling approach, to assess the 'normativeness' of neuroanatomical profiles in individuals at CHR-P. CHR-P individuals demonstrated no greater regional heterogeneity after applying FDR corrections. However, PBSI scores indicated significantly greater neuroanatomical divergence in global SA, CT and SV profiles in CHR-P individuals compared with HC. Normative PBSI analysis identified 11 CHR-P individuals (0.70%) with marked deviation (>1.5 SD) in SA, 118 (7.47%) in CT and 161 (10.20%) in SV. Psychosis transition was not significantly associated with any measure of heterogeneity. Overall, our examination of neuroanatomical heterogeneity within the CHR-P state indicated greater divergence in neuroanatomical profiles at an individual level, irrespective of psychosis conversion. Further large-scale investigations are required of those who demonstrate marked deviation.

Translational Psychiatry (2022)12:297; <https://doi.org/10.1038/s41398-022-02057-y>

INTRODUCTION

The Clinical High-Risk state for Psychosis (CHR-P) [1] describes individuals who are at an increased risk of later developing psychosis and can benefit from early intervention, usually implemented in specialised clinics that are emerging worldwide [2, 3]. Individuals at CHR-P accumulate various risk factors for psychosis [4, 5] and have about 50-fold increased risk of transitioning to a first episode of psychosis (FEP) compared to healthy controls (HC) [6]. The CHR-P state consists of several subgroups, each with varying clinical profiles: Attenuated Psychotic Symptoms (APS), Brief Limited Intermittent Psychotic Symptoms (BLIPS) and/or genetic vulnerability accompanied by a deterioration in functioning (GRD) [7–9]. Furthermore, individuals at CHR-P have a highly variable risk enrichment [10] and substantial clinical heterogeneity in initial symptoms, functional status, transition to psychosis, and remission or persistence of symptoms [11–16]. In fact, this observed heterogeneity in clinical and outcome features has been a source of ongoing criticism of the CHR-P paradigm [17, 18]. Such heterogeneity poses a challenge to determining treatment responsiveness and the prediction of longitudinal outcomes.

Substantial research efforts have focused on the identification of neuroanatomical abnormalities in individuals at CHR-P, investigated with structural magnetic resonance imaging (sMRI)

[19–24]. For example, the Enhancing Neuroimaging Genetics through Meta-Analysis (ENIGMA) [25] consortium recently established the CHR-P Working Group [20] offering the largest pooled structural neuroimaging CHR-P dataset to date. The working group identified widespread deficits in cortical thickness in those at CHR-P compared with HC, which was associated with a transition to psychosis [20]. As such, there have been similar efforts to harness the findings of neuroanatomical deficits to improve the detection of cases and the prediction of transition to FEP [26–28]. However, to date, no reliable neuroanatomical biomarkers have been established, raising the hypothesis of underlying heterogeneity in MRI-based estimates of morphometry and associated neurobiological profiles within the CHR-P state [29, 30].

Emerging statistical measures have made it easier to investigate group-level or personalised estimates of variability in neuroanatomical measures. Heterogeneity within specific anatomical regions can be quantified using the Variability Ratio (VR) or Coefficient of Variation (CV) ratio [31], which have been used to demonstrate greater group-level variability (i.e. heterogeneity) in volumetric measures of the putamen, temporal lobe, thalamus and third ventricle, and lower variability (i.e. homogeneity) in the anterior cingulate cortex of patients with schizophrenia compared to HC [32]. Furthermore, a recent meta-analysis that investigated

A full list of authors and their affiliations appears at the end of the paper.

Received: 24 May 2022 Revised: 28 June 2022 Accepted: 1 July 2022

Published online: 26 July 2022

variability across a narrow subset of structural volumetric brain regions, indexed with the VR, reported no significant differences between individuals at CHR-P and HC, or between those who subsequently transitioned to psychosis and those who did not [33]. Taken together, these findings suggest that variability, as measured by VR, is not significantly different in CHR-P vs. HC.

However, these results stand in contrast to studies that use alternative indices of variability. The Person-Based Similarity Index (PBSI) yields a personalised metric representing inter-subject correlations of neuroanatomical profiles [34–36], and has received recent attention in the context of psychiatric samples, including individuals with bipolar disorder [35, 36] and schizophrenia [36]. The PBSI was recently compared between CHR-P ($n = 71$), FEP ($n = 72$) and HC ($n = 55$) [37], revealing heterogeneity at a personalised level in CHR-P samples. Further, those demonstrating the most marked deviation also demonstrated generally lower IQ and poorer psychopathology [37]. These findings are in contrast with the former meta-analytic findings [33]. However, these incongruities may be explained by the discrepant indices applied, the narrow focus of the brain regions studied meta-analytically [33] and/or the relatively small sample recruited for the PBSI investigations [37]. Taken together, the existing literature offers an ambiguous picture of neuroanatomical heterogeneity in the CHR-P state; as such, further investigations are warranted.

The rationale for elucidating neuroanatomical heterogeneity in the context of CHR is four-fold. First, by examining neuroanatomical heterogeneity in CHR-P, we will gain a fuller understanding of neuroanatomy of the CHR-P population, which allows us to better address criticisms of the CHR-P paradigm which often centre around heterogeneity. Then, this increased understanding may inform the development of precision and predictive models of psychosis. Third, modelling neuroanatomical heterogeneity offers a unique opportunity to identify individuals with potentially shared characteristics of importance. Finally, through subgroup investigations stratified by clinical features, such as a transition to psychosis status and subgroup status (i.e. APS/BLIPS/GRD), we could identify clinical relevance associated with neuroanatomical heterogeneity.

The ENIGMA [25] consortium offers rich structural neuroimaging data across a diverse sample at CHR-P [20], and therefore presents a unique opportunity to systematically address the issue of heterogeneity in this population. Here, we aimed to apply both group-level and personalised indices to investigate whether neuroanatomical heterogeneity differed significantly between; (i) individuals at CHR-P and HC, and (ii) individuals at CHR-P who subsequently transitioned to psychosis and those who did not. In line with the widely reported significant differences between CHR-P and HC in mean neuroanatomical measures, we hypothesised that variance will also significantly differ between the two groups. This assumption is directed by the observation of heightened heterogeneity in other aspects of the CHR-P paradigm, the current lack of successful biomarkers in the CHR-P field and the corresponding potential for discrepant underpinning neurobiological processes. Specifically, we hypothesised that individuals at CHR-P will demonstrate significantly increased heterogeneity in neuroanatomical measures, as demonstrated by significantly higher VR effect sizes and significantly lower PBSI scores.

METHODS

This study was conducted according to the Reporting of studies Conducted using Observational Routinely-collected health Data (RECORD) Statement [38] (eTable 1).

Participants

The ENIGMA CHR-P dataset amalgamated clinical and neuroimaging data from 29 sites, comprising 1579 individuals meeting CHR-P criteria (according to Comprehensive Assessment of At-Risk Mental States

[CAARMS] [9] or the Structured Interview for Prodromal Syndromes [SIPS] [39, 40]) and 1243 HC participants. Longitudinal clinical data that measured transition to psychosis, were also recorded (transition rate [$n = 226$, 14.31%], follow-up duration in months [mean = 28.07, SD = 32.50]). Each site obtained ethics committee approval prior to data collection, and participants provided informed consent or assent prior to participation. Further participant inclusion and exclusion criteria have been previously described [20], and sample discrepancies with the original ENIGMA CHR-P study are detailed in eFig. 1.

MRI data acquisition and processing

The site-specific MRI data acquisition parameters are summarised in eTable 2. All neuroimaging data were processed according to FreeSurfer automated pipelines [41–44] and the standardised ENIGMA protocol (<http://enigma.ini.usc.edu/protocols/imaging-protocols/>). Briefly, the FreeSurfer pipeline includes motion correction, automated Talairach transformation [45], skull stripping [46], segmentation of the sub-cortical white matter and grey matter volumetric structures [43, 47], and intensity normalisation [48]. The ENIGMA quality control procedure identifies outliers (± 2 SD from the mean) and includes a visual inspection of all images to remove poorly segmented regions, thus resulting in minor fluctuation in sample size for each region of interest (ROI). The application of this protocol yielded a total of 153 structural ROIs: 68 cortical variables measured by both Surface Area (SA) and Cortical Thickness (CT) according to the Desikan–Killiany atlas [49], 16 Subcortical Volume (SV) variables and one measure of Intracranial Volume (ICV). Participants with >5% missing ROIs were excluded from the current analyses as this was deemed to be indicative of poor parcellation (eFig. 1).

Neuroimaging data were adjusted for scanner protocol and site using neuroComBat [50] (a modified version of ComBat [51]), a batch-adjustment method that relies on an empirical Bayes framework to assess the influence of covariates of interest. The neuroimaging data were adjusted prior to current analyses, as this approach is recommended by the tool developers for optimal use while controlling for group (CHR-P/HC), age and sex. NeuroComBat has previously been validated on data derived from the ENIGMA protocol described above (in the ENIGMA SCZ dataset) [52] and allows for partially missing data [50]. In previous work using this dataset, we have empirically demonstrated that applying neuroComBat to the data reported here leads to more precise estimates of effect sizes, both compared to non-neuroComBat-corrected data and random-effects meta-analysis [20].

Statistical analysis

All analyses were conducted within *R* v.4.0.3 [53]; the VR analyses were conducted using the *metafor* [54] and *meta* [55] packages. Effect sizes were previously reported for group differences in each ROI between CHR-P/HC and transition status [20]; as such, the current analysis provides an in-depth exploration of neuroanatomical heterogeneity in this dataset using baseline clinical and neuroimaging data and longitudinal clinical outcome data.

Variability ratio and coefficient of variation. We applied the log-VR using the *escal()* function; this statistical index has gained recent attention as an indicator of inter-individual variability for various clinical factors, such as treatment effect [31, 56], and is calculated according to the formula below:

$$\ln \text{VR} = \ln \left(\frac{\hat{\sigma}_p}{\hat{\sigma}_c} \right) = \ln \left(\frac{S_p}{S_c} \right) + \frac{1}{2(n_p - 1)} - \frac{1}{2(n_c - 1)}$$

where $\hat{\sigma}_p$ and $\hat{\sigma}_c$ are the unbiased estimates of population SDs; S_p and S_c are the reported sample SDs; n_p and n_c are the sample sizes for CHR-P (or CHR-T/APS) and HC (or CHR-NT) groups, respectively.

This calculation was conducted across each ROI to compare baseline variability in regional neuroanatomical measures between CHR-P and HC in the first instance, and then between CHR-P individuals who transitioned to FEP (CHR-T) and those who did not (CHR-NT). CHR-P participants who were lost to follow-up ($n = 258$) were not included in the latter investigation (eFig. 1). We also conducted further exploratory applications limited to those meeting APS subgroup criteria compared with HC. Due to the low prevalence of the BLIPS and GRD subgroups (see Table 1) and the corresponding high volume of ROIs under investigation, it was not feasible to conduct analyses limited to these two subgroups, respectively.

Table 1. Sample characteristics for the clinical-high risk for psychosis (CHR-P) and the healthy control (HC) groups.

	CHR-P (N = 1579)	HC (N = 1243)
Age in years, mean (SD)	20.63 (4.60)	22.32 (4.96)
Sex, M/F	831/748	687/556
Transition to psychosis, %	14.31	NA
Follow-up duration in months, mean (SD)	28.07 (32.50)	NA
Typical antipsychotics, n (%)	15 (0.95%)	NA
Atypical antipsychotics, n (%)	216 (13.68%)	NA
Total severity symptoms score ^a , mean (SD)	CAARMS: 10.34 (4.03) SIPS: 10.93 (4.66)	NA
Subgroups ^b , n (%)	APS: 1177 (74.54%) BLIPS: 46 (2.91%) GRD: 90 (5.70%) APS/GRD: 129 (8.17%) APS/BLIPS: 27 (1.71%) BLIPS/GRD: 2 (0.13%%) APS/BLIPS/GRD: 7 (0.44%) Unknown: 101 (6.40%%)	NA

^a243 participants had neither the CAARMS nor SIPS assessment scores provided.

^bAPS Attenuated Psychotic Symptoms; BLIPS Brief Limited Intermittent Psychotic Symptoms; GRD Genetic and Risk Deterioration Syndrome; some participants met criteria for more than one subgroup.

The log-VR was back-transformed into linear scale (VR) to aid interpretation of the results. Therefore, a VR of 1 indicates equal variability in neuroanatomical measures between groups. A VR > 1 suggests greater variability in the CHR-P group (or CHR-T and APS, respectively), whereas a VR < 1 indicates less variability in the CHR-P group. The VR (with 95% confidence intervals) for each ROI were then summarised in forest plots according to SA, CT, SV and ICV. Given the high number of ROI tests conducted, we calculated *p* value adjustments using the False Discovery Rate (FDR) [57] approach, applied to all of the ROIs as one vector at once. As such, the forest plots report both the uncorrected and corrected *p*-values.

Previous research within the ENIGMA CHR dataset identified between-group mean differences of sMRI measures [20]. As the log variability ratio (log-VR) is not scaled to the mean, we conducted a supplementary calculation of the log Coefficient of Variation (log-CV) ratio index, which offers a mean-scaled metric of variability between two groups and is calculated according to the formula below [31]. In instances in which the CHR-P population (or CHR-T/APS groups) demonstrate lower mean sMRI values compared with the HC population (or CHR-NT), the log-VR offers the more conservative test of our hypotheses. However, in instances of larger mean values in the CHR-P population or the transition to psychosis group, the log-CV offers the more conservative test. As previous research in this data set largely described lower mean values across sMRI measures in the CHR-P population, particularly regarding measures of CT [20], we calculated the log-CV to supplement the findings of the primary log-VR analyses.

$$\ln \text{CVR} = \ln \left(\frac{\hat{\sigma}_p / \bar{x}_p}{\hat{\sigma}_c / \bar{x}_c} \right) = \ln \left(\frac{S_p / \bar{x}_p}{S_c / \bar{x}_c} \right) + \frac{1}{2(n_p - 1)} - \frac{1}{2(n_c - 1)}$$

where \bar{x}_p and \bar{x}_c are the reported means for the CHR-P (or CHR-T/APS) and HC (or CHR-NT) groups.

Finally, we conducted sensitivity analyses on ROIs demonstrating significant effects in the primary analyses, to better elucidate whether identified effects might be better explained in part by factors associated with suboptimal study design as opposed to meaningful neurobiological mechanisms. These analyses included leave-one-out resampling to investigate site effects (eMethods 1), and supplementary testing on an age-, sex-, and site-matched sample (eMethods 2) to control for other potential sources of heterogeneity.

Person-Based Similarity Index. The personalised estimates of inter-individual variability were investigated using the PBSI, calculated according to the formula below, for each SA, CT and SV profiles [34–37]. The process for calculating the PBSI scores begins with concatenating the respective regional measures into vectors that represent the profile of each specific brain phenotype; PBSI-SA, PBSI-CT and PBSI-SV, respectively. This produces

a simplified, personalised index for each phenotypic neuroanatomical profile. This index can then be used in one of two ways; first, to quantify how similar an individuals' brain profile is to that of other individuals with the same clinical profile or disorder (within-diagnosis or within-group). Second, to quantify how similar an individuals' brain profile is relative to a normative estimate, i.e. the average of the healthy control group (normativeness) [37].

$$\text{PBSI}_i = \frac{1}{N-1} \sum_{j \neq i} \text{cor}(y_i, y_j)$$

The PBSI of the *i*th individual is the average correlation between his/her brain measures (y_i) and the brain measures of any other individual of the reference sample (y_j , for $j \neq i$).

- (i) *Within-group reference:* The PBSI-SA, PBSI-CT and PBSI-SV were calculated separately for the CHR-P and HC individuals and thus represent the degree of within-group similarity in these profiles. Within each group, and for each brain phenotype, Spearman correlation coefficients were computed between the neuroanatomical profile of each participant and the profiles of each other member of the same group. The average of these coefficients for each participant yielded their respective PBSI score for each brain phenotype. A higher PBSI score (closer to 1) indicates greater similarity in the neuroanatomical profile of an individual to other members of the same group, while a lower score indicates greater deviance in their neuroanatomical profile. Group-level comparisons of PBSI-SA, PBSI-CT and PBSI-SV were then conducted between CHR-P and HC using one-tailed Welch's *t* tests to examine whether psychosis-risk states were associated with greater within-group variability.
- (ii) *Normative reference:* Next, the respective neuroanatomical profiles of each CHR-P individual were correlated with the corresponding profiles of the members of the HC group, for each brain phenotype. The resulting PBSI scores thus represent the degree of deviation from the 'normative' range and were transformed into *z*-scores (PBSI-CT-Z, PBSI-SA-Z, and PBSI-SV-Z). We set >1.5 SD as a threshold to identify individuals at CHR-P who most markedly deviated from the normative neuroanatomical profile, in line with previous work [37].

In both PBSI analyses, we also investigated the potentially moderating effects of transition status (CHR-T/CHR-NT), subgroup status (APS/BLIPS/GRD), antipsychotic exposure, and overall baseline psychopathology (total CAARMS/SIPS severity *z*-scores, eMethods 3) on PBSI scores. All multi-variable regression models were applied, adjusting for age and sex.

RESULTS

Sample characteristics

Following quality control procedures (eFig. 1), the final sample consisted of 1 579 CHR-P participants (mean age = 20.63 [SD = 4.60], 47.37% females) and 1243 HC participants (mean age = 22.32 [SD = 4.96], 44.73% females) across 29 sites. Table 1 provides a detailed sample summary. Of the CHR-P participants, 1248 also had longitudinal clinical data; the length of follow-up ranged from 1 to 194 months (mean = 28.07 [SD = 32.50], median = 18.00). eTable 3 provides a detailed comparison of the CHR-T and CHR-NT groups.

Variability ratio and coefficient of variation

CHR-P compared with HC

Regional SA: While the CHR-P group demonstrated a trend towards greater variability compared to the HC group in measures of cortical SA in the right lateral orbitofrontal region (VR = 1.08, 95% CI: 1.02–1.14), left lateral orbitofrontal region (VR = 1.08, 95% CI: 1.02–1.13) and right rostral middle-frontal region (VR = 1.07, 95% CI: 1.02–1.13), these observations did not survive FDR adjustments. No SA regions demonstrated significantly greater homogeneity in CHR-P (Fig. 1). These trends were confirmed in CV analyses (eFig. 2).

Regional CT: There was a trend towards greater heterogeneity in CHR-P compared to HC in the right cuneus (VR = 1.08, 95% CI: 1.03–1.14), right inferior-temporal region (VR = 1.08, 95% CI: 1.02–1.14), left middle-temporal region (VR = 1.07, 95% CI: 1.02–1.13), right precentral region (VR = 1.07, 95% CI: 1.00–1.15, $p = 0.01$) and left pars opercularis (VR = 1.07, 95% CI: 1.02–1.13). Again, these observations did not remain statistically significant after applying FDR corrections. No regions demonstrated greater homogeneity in CHR-P compared to HC (Fig. 2). Supplementary CV analyses (eFig. 3) supported these findings.

Regional SV: There was a numerical trend towards higher heterogeneity in CHR-P compared to HC individuals in the left hippocampus (VR = 1.07, 95% CI: 1.01–1.13), notwithstanding FDR corrections (Fig. 3). Supplementary CV (eFig. 4) analyses corroborated these findings.

ICV: No significant differences in ICV heterogeneity or homogeneity were observed between CHR-P and HC, indexed with either the VR (eFig. 5) or CV (eFig. 6).

CHR-T compared with CHR-NT. CHR-P individuals who transitioned to psychosis did not demonstrate significantly greater heterogeneity or homogeneity in regional neuroanatomical measures compared with individuals who did not transition to psychosis, as indexed by both the VR and CV (eFigs. 7–14).

APS compared with HC. Individuals meeting the criteria for the APS subtype demonstrated a trend towards greater SA heterogeneity in the left lateral orbitofrontal region (VR = 1.07, 95% CI: 1.01–1.14) compared with HC (eFig. 15), but no regions survived FDR correction for multiple comparisons. No other significant regions were identified in VR or CV analyses (eFigs. 16–22).

Person-Based Similarity Index

Within-group PBSI. There was greater within-group variability in all neuroanatomical profiles in the CHR-P group compared to the HC group based on significantly lower PBSI-SA ($t(2642) = -5.39$, $p < 0.01$), PBSI-CT ($t(2788) = -9.11$, $p < 0.01$), and PBSI-SV scores ($t(2733) = -4.34$, $p < 0.01$) (Fig. 4). PBSI-CT scores were substantially lower than PBSI-SA and PBSI-SV (Fig. 4), signalling greater divergence specifically in CT profiles. There were no significant associations between PBSI scores and transition or subgroup status, baseline psychopathology (all $p > 0.12$), or current typical or atypical antipsychotic use on PBSI-SA or PBSI-CT scores. There was

a slight association of typical antipsychotic use with PBSI-SV scores, albeit not surviving the stricter significance threshold ($b = -0.02$, $t(1220) = -2.017$, $p = 0.04$).

Normative PBSI. Of the 1579 CHR-P participants, 11 (0.70%) demonstrated marked deviation in PBSI-SA-Z scores, 118 (7.47%) in PBSI-CT-Z and 161 (10.20%) in PBSI-SV-Z (Fig. 5). Of these participants, 17 demonstrated marked deviation in more than one phenotypic profile and just one participant in all three phenotypic profiles. There were no significant associations between normative PBSI scores and transition or subgroup status, or baseline psychopathology (all $p > 0.18$). A significant association with typical antipsychotic use was identified for the PBSI-SV-Z scores ($b = -0.84$, $t(1220) = -2.191$, $p = 0.03$), with antipsychotic use being associated with greater deviations from PBSI-SV-Z. No association with antipsychotic use was identified with PBSI-SA-Z or PBSI-CT-Z scores.

DISCUSSION

We conducted a large-scale investigation of neuroanatomical heterogeneity in a help-seeking population meeting CHR-P criteria. To summarise, we observed a trend towards regional heterogeneity (as measured by the variability ratio) in a cluster of frontal, temporal and hippocampal regions that failed to reach statistical significance after correction for multiple comparisons. However, Person-Based Similarity Index (PBSI) analyses, a novel measure of inter-individual variability, indicated greater divergence in global neuroanatomical profiles of SA, CT and SV in CHR-P compared with HC. Importantly, however, the proportion of CHR-P individuals with significantly deviant PBSI scores was low. Moreover, none of the variability metrics examined showed significant associations with a transition to psychosis.

Our first key finding was an observed trend towards heightened heterogeneity in individuals at CHR-P in a cluster of frontal, temporal and hippocampal regions compared with HC. This result is in line with the fine-grained and localised alterations typically observed in the CHR-P state. Existing literature has identified structural, [26, 58–60] functional [26, 60], and neurocognitive [61] alterations in frontal and medial-frontal regions in the CHR-P state, [26, 58–60] and further highlighted these as potentially important regions in the pathophysiology of psychosis. [26, 58–60] Similarly, aberrations in temporal [26, 59, 60, 62] and hippocampal regions [26, 59, 63–66] have also been identified in CHR-P and have been implicated as core regions in the transition to psychosis. To observe localised heterogeneity in these regions might signal discrepant neurobiological processes associated with psychosis-risk states (or with psychosis conversion in subsequent CHR-T/CHR-NT analyses), which may ultimately prove useful for stratification purposes in interventional research. However, all observed effect sizes were small (1.06–1.08) and these findings did not survive the FDR correction for multiple comparisons. Furthermore, no significant effects of the transition to psychosis were identified. These results are consistent with a recent meta-analysis that applied the VR across a smaller subset of volumetric regions and similarly identified no significant regions of increased variability in CHR-P [33]. Equally, a previous study that compared CHR-P ($n = 71$) and HC ($n = 55$), indexed with the CV metric, found no evidence of regional increases in variability in CHR-P [37], demonstrating the robustness of these findings. Taken together, these findings, in combination with ours, suggest that regional neuroanatomical variability in the CHR-P state is not significantly different from healthy controls.

However, the application of the PBSI offered a somewhat contrasting conclusion. The within-diagnosis PBSI estimates revealed significantly lower scores across global SA, CT and SV amongst individuals at CHR-P, compared with HC. These findings signal greater divergence in neuroanatomical profiles within the CHR-P state across all three phenotypic measures. This finding is largely consistent with previous research which identified lower

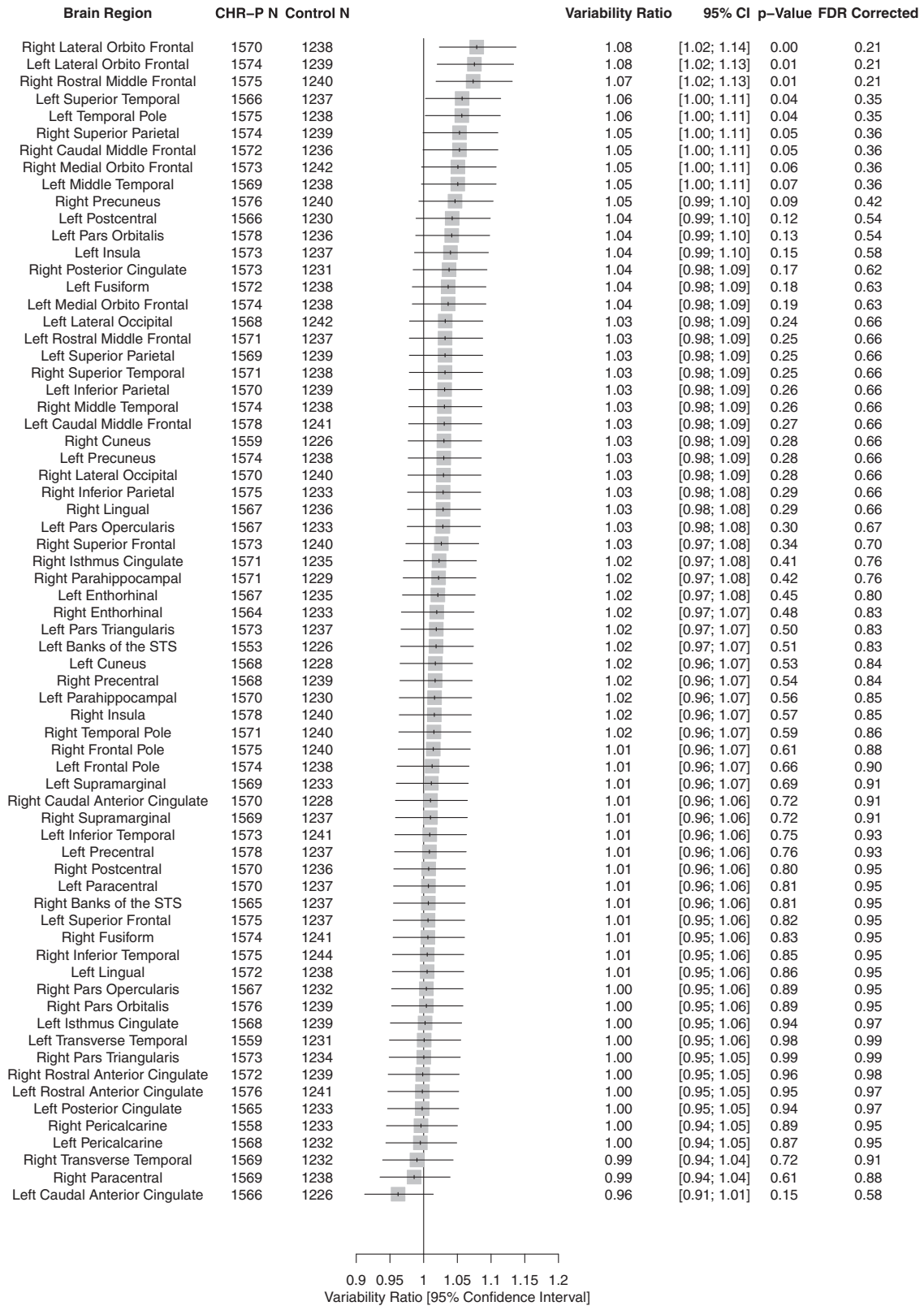


Fig. 1 Forest plot of the variability ratio (VR) of cortical surface area (SA) measures in CHR-P compared with healthy controls. CHR-P clinical high risk for psychosis, STS superior temporal sulcus, VR variability ratio.

PBSI-CT and PBSI-SV scores in individuals at CHR-P compared with HC [37]. Notably, higher variability in CT profiles was also reported in another sample of patients with schizophrenia compared to HC [36]. These findings suggest that higher inter-individual variability

in cortical and subcortical phenotypes is a consistent feature both at the at-risk stage and after the onset of FEP. This is also particularly interesting within the context of previous findings in the ENIGMA CHR-P dataset of widespread CT deficits [20], and

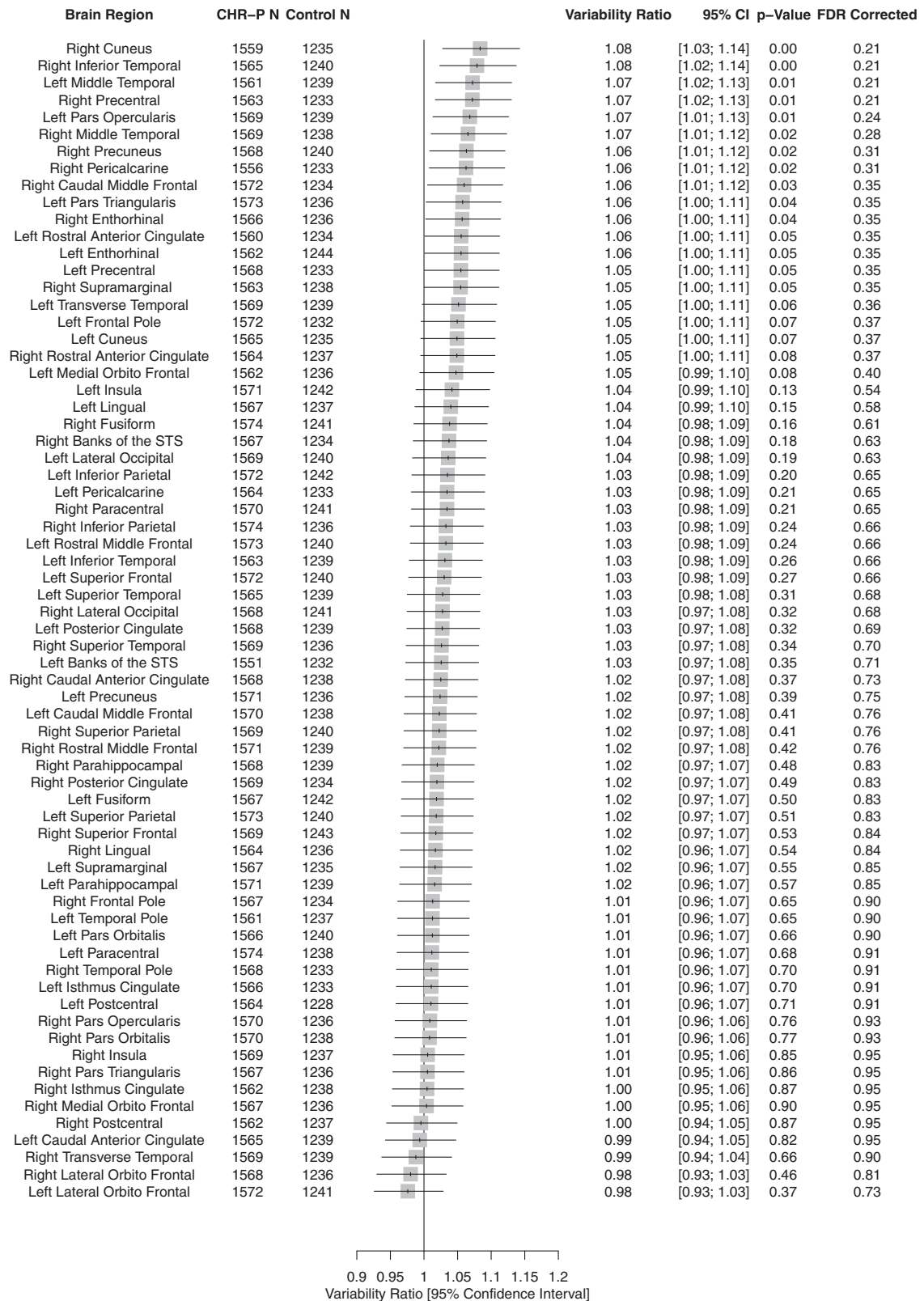


Fig. 2 Forest plot of the variability ratio (VR) of cortical thickness (CT) measures in CHR-P compared with healthy controls. CHR-P clinical high risk for psychosis, STS superior temporal sulcus, VR variability ratio.

warrants further investigation of variance specifically in CT phenotypes across the psychosis spectrum.

Crucially, normative modelling of the PBSI also identified a sub-sample of CHR-P individuals who demonstrated marked deviation

in reference to a 'normative' neuroanatomical profile. The identification of deviations from normative modelling is becoming increasingly popular in psychiatry and may aid in the classification of distinct subgroups. [35–37, 67] Although <1% of the sample

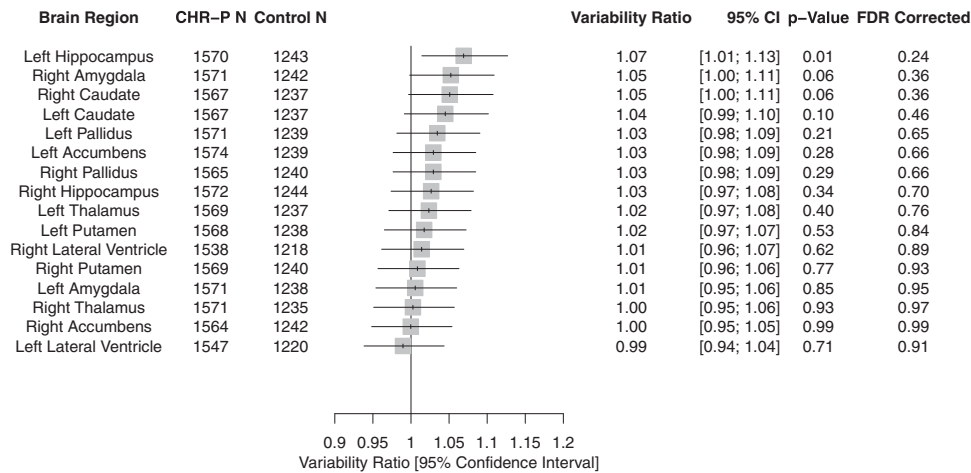


Fig. 3 Forest plot of the variability ratio (VR) of subcortical volume (SV) measures in CHR-P compared with healthy controls. CHR-P clinical high risk for psychosis, VR variability ratio.

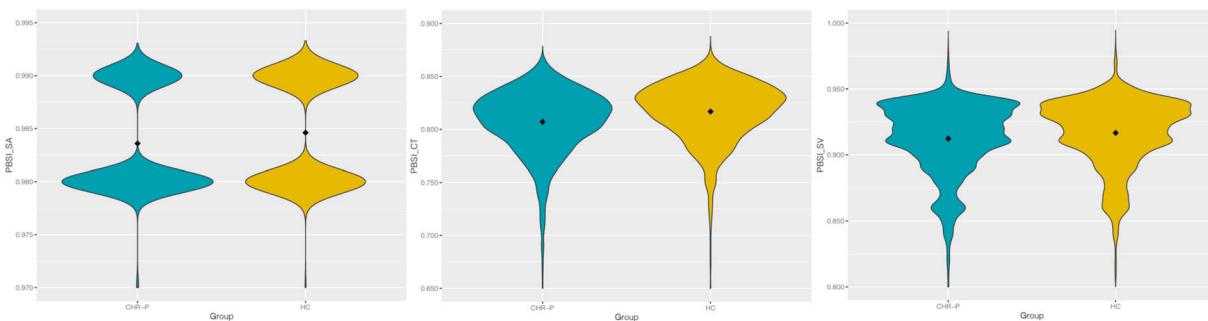


Fig. 4 Violin plots comparing the distribution of PBSI scores between individuals at CHR-P and healthy controls, across surface area (PBSI_SA), cortical thickness (PBSI_CT), and subcortical volume (PBSI_SV); the mid-point indicates the group mean. PBSI Person-Based Similarity Index, SA surface area, CT cortical thickness, SV subcortical volume. All three phenotypes demonstrate significantly lower similarity in PBSI profiles in the CHR-P group compared with healthy controls, across PBSI_SA ($p < 0.01$), PBSI_CT ($p < 0.01$), PBSI_SV ($p < 0.01$).

displayed markedly 'deviant' PBSI-SA scores, this rose to 7.47% for PBSI-CT and 10.20% for PBSI-SV scores, suggesting that approximately 7–10 out of 100 CHR-P individuals have markedly deviant neuroanatomical profiles in SV or CT compared to HC. Together, the PBSI findings indicate the potential utility of examining personalised indexes as opposed to employing group-level estimations of variance. However, the observed heterogeneity in CHR-P individuals was not significantly associated with severity of baseline attenuated psychotic psychopathology, subgroup allocation (APS/BLIPS/GRD) or transition to psychosis. These findings suggest that neuroanatomical variability is not linked to the clinical features we examined.

The lack of an association between heterogeneity and transition to psychosis may reflect the challenges we face when employing dichotomous diagnostic criteria—particularly as psychosis risk is associated with various transdiagnostic outcomes [16]. At this time, we were unable to assess the link between neuroanatomical heterogeneity and other longitudinal clinical outcomes, such as psychosocial functioning, non-psychotic psychopathology or persistence of attenuated symptoms. However, harmonisation of additional outcome measures is an ongoing endeavour of the ENIGMA CHR working group; therefore, in the future, we plan to examine how neuroanatomical heterogeneity is associated with other measures. Given the prevalence and variability of these alternative outcomes in the CHR-P state [68–70], it will be important to assess whether these hold greater associations with neuroanatomical variability in order to better address the clinical relevance of neuroanatomical heterogeneity. In this respect, it may be especially pertinent to investigate the subgroup of

individuals at CHR-P who markedly deviated from the 'norm' in the PBSI analyses. Furthermore, there was substantial variation in follow-up duration between sites. As such, it is possible that the presence of individuals at CHR-P that were classified as 'no transition'—yet who may have developed psychosis following their final data contributions—may have reduced our power to detect group differences.

There are also further methodological limitations to consider. First, the validity of the VR as an index of heterogeneity has been debated, particularly within the context of other clinical factors, such as individual treatment response and subgroup effects [71]. While we performed additional individual-level PBSI analyses to supplement the VR analyses, the indices produced somewhat conceptually discrepant findings. These discrepancies may be underpinned by the group-level approach of the VR index as opposed to the individual-level PBSI scores, or alternatively due to the nature of the PBSI scores which capture overall patterns of neuroanatomical heterogeneity as opposed to specific regional patterns. It is possible that adopting a global approach offers a more powerful examination of heterogeneity compared to a region-by-region approach. Nevertheless, these current findings corroborate existing literature which reported significant differences in variability of neuroanatomical profiles with the application of PBSI scores [37], and a lack thereof with a regional group-level VR [33] or CV [37] approach. However, the current findings also necessitate further validation and critical appraisal of the various indices of heterogeneity. Heterogeneity has recently become a mainstay focus of clinical research—particularly in psychiatry—and it is imperative to systematically compare the

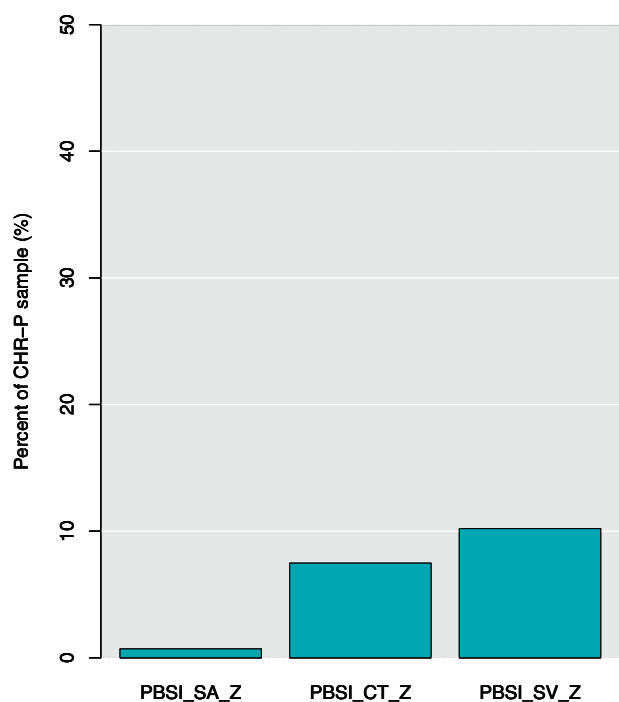


Fig. 5 A bar chart representing the percentage of the CHR-P sample who demonstrate marked deviation from the 'normative' neuroanatomical profile. CHR-P clinical high risk for psychosis, PBSI_SA_Z person-based similarity index surface area z-scores, PBSI_CT_Z person-based similarity index cortical thickness z-scores, PBSI_SV_Z person-based similarity index subcortical volume z-scores.

statistical performance of the relevant indices in order to develop a gold standard framework for addressing questions of variance.

Second, we were also unable to control for further potentially confounding factors, such as substance use. Given the potential impact of alcohol, tobacco and cannabis use on neuroanatomical profiles in CHR-P [72, 73], it will be important to assess these features as this consortium continues to develop and expand. Future research should also continue to explore heterogeneity within the CHR-P paradigm, both within neurobiological bases and other characteristics. The elucidation of such sources of heterogeneity will be essential in order to improve prognostic research paradigms in this population [74].

Future directions

Given these limitations, there is a range of next steps to further elucidate neuroanatomical heterogeneity in the CHR-P paradigm. First, as the ENIGMA CHR-P Working Group continues to develop and expand, it would be interesting to incorporate genomic data to assess the genetic contributions to population variability in neuroimaging phenotypes, such as the schizophrenia polygenic risk score [75], as well as assessing the association of neuroanatomical heterogeneity with alternative clinical and functional outcomes outside of transition to psychosis. Finally, once longitudinal neuroimaging data becomes available, it will also be important to assess the longitudinal stability of the neuroanatomical heterogeneity findings here.

CONCLUSIONS

In the largest pooled neuroimaging sample of individuals at CHR-P to date, we identified an absence of significantly greater regional heterogeneity compared with HC, despite an emerging trend towards greater fronto-temporal and hippocampal heterogeneity

in CHR-P. These findings persist irrespective of longitudinal transition to psychosis. Subsequent application of a personalised PBSI score revealed significantly greater divergence in global neuroanatomical profiles in CHR-P, and further, a small subgroup (approximately 10%) of individuals at CHR-P who demonstrate markedly divergent neuroanatomical profiles of SA, CT and SV respective to a normative profile. Further clinical investigation of this subgroup is required in light of the limited clinical variables currently available.

CODE AVAILABILITY

Computer code to calculate the VR, CVR and PBSI statistics is available from the authors upon request.

REFERENCES

- Fusar-Poli P. The Clinical High-Risk State for Psychosis (CHR-P), Version II. *Schizophr Bull.* 2017;43:44–7.
- Kotlicka-Antczak M, Podgórski M, Oliver D, Maric NP, Valmaggia L, Fusar-Poli P. Worldwide implementation of clinical services for the prevention of psychosis: the IEPA early intervention in mental health survey. *Early Inter Psychiatry.* 2020;14:741–50.
- Salazar de Pablo G, Estradé A, Cutroni M, Andlauer O, Fusar-Poli P. Establishing a clinical service to prevent psychosis: what, how and when? *Systematic review. Transl Psychiatry.* 2021;11:43.
- Fusar-Poli P, Tantardini M, De Simone S, Ramella-Cravaro V, Oliver D, Kingdon J, et al. Deconstructing vulnerability for psychosis: meta-analysis of environmental risk factors for psychosis in subjects at ultra high-risk. *Eur Psychiatry.* 2017;40:65–75.
- Radua J, Ramella-Cravaro V, Ioannidis JPA, Reichenberg A, Phipphothatsanee N, Amir T, et al. What causes psychosis? An umbrella review of risk and protective factors. *World Psychiatry.* 2018;17:49–66.
- Salazar de Pablo G, Radua J, Pereira J, Bonoldi I, Arienti V, Besana F, et al. Probability of Transition to psychosis in individuals at clinical high risk: an updated meta-analysis. *JAMA Psychiatry.* 2021;78:970.
- Catalan A, Salazar de Pablo G, Vaquerizo Serrano J, Mosillo P, Baldwin H, Fernández-Rivas A, et al. Annual Research Review: Prevention of psychosis in adolescents - systematic review and meta-analysis of advances in detection, prognosis and intervention. *J Child Psychol Psychiatry.* 2020;62:657–73.
- Fusar-Poli P, Salazar de Pablo G, Correll CU, Meyer-Lindenberg A, Millan MJ, Borgwardt S, et al. Prevention of psychosis: advances in detection, prognosis, and intervention. *JAMA Psychiatry.* 2020;77:755.
- Yung AR, Yung AR, Pan Yuen H, McGorry PD, Phillips LJ, Kelly D, et al. Mapping the onset of psychosis: the comprehensive assessment of at-risk mental states. *Aust NZ J Psychiatry.* 2005;39:964–71.
- Fusar-Poli P, Schultze-Lutter F, Cappucciati M, Rutigliano G, Bonoldi I, Stahl D, et al. The dark side of the moon: meta-analytical impact of recruitment strategies on risk enrichment in the clinical high risk state for psychosis. *Schizophr Bull.* 2016;42:732–43.
- Fusar-Poli P, Cappucciati M, Bonoldi I, Hui LMC, Rutigliano G, Stahl DR, et al. Prognosis of brief psychotic episodes: a meta-analysis. *JAMA Psychiatry.* 2016;73:211.
- Fusar-Poli P, Cappucciati M, Borgwardt S, Woods SW, Addington J, Nelson B, et al. Heterogeneity of psychosis risk within individuals at clinical high risk: a meta-analytical stratification. *JAMA Psychiatry.* 2016;73:113.
- Fusar-Poli P, De Micheli A, Chalambrides M, Singh A, Augusto C, McGuire P. Unmet needs for treatment in 102 individuals with brief and limited intermittent psychotic symptoms (BLIPS): implications for current clinical recommendations. *Epidemiol Psychiatr Sci.* 2020;29:e67.
- Fusar-Poli P, De Micheli A, Signorini L, Baldwin H, de Pablo GS, McGuire P. Real-world long-term outcomes in individuals at clinical risk for psychosis: the case for extending duration of care. *EclinicalMedicine.* 2020;28:100578.
- Fusar-Poli P, Salazar de Pablo G, Rajkumar RP, López-Díaz Á, Malhotra S, Heckers S, et al. Diagnosis, prognosis and treatment of brief psychotic episodes: a review and research agenda. *Lancet Psychiatry.* 2022;9:72–83.
- Rutigliano G, Valmaggia L, Landi P, Frascarelli M, Cappucciati M, Sear V, et al. Persistence or recurrence of non-psychotic comorbid mental disorders associated with 6-year poor functional outcomes in patients at ultra high risk for psychosis. *J Affect Disord.* 2016;203:101–10.
- van Os J, Guloksuz S. A critique of the 'ultra-high risk' and 'transition' paradigm. *World Psychiatry J.* 2017;16:200–6.
- Malhi GS, Bell E, Hamilton A, Morris G. Early intervention for risk syndromes: what are the real risks? *Schizophr Res.* 2021;227:4–9.

19. Brent BK, Thermenos HW, Keshavan MS, Seidman LJ. Gray matter alterations in schizophrenia high-risk youth and early-onset schizophrenia. *Child Adolesc Psychiatr Clin N Am* 2013;22:689–714.
20. ENIGMA Clinical High Risk for Psychosis Working Group, Jalbrzikowski M, Hayes RA, Wood SJ, Nordholm D, Zhou JH, et al. Association of structural magnetic resonance imaging measures with psychosis onset in individuals at clinical high risk for developing psychosis: An ENIGMA Working Group Mega-analysis. *JAMA Psychiatry*. 2021;78:753.
21. Koutsouleris N, Schmitt GJE, Gaser C, Bottlender R, Scheuerecker J, McGuire P, et al. Neuroanatomical correlates of different vulnerability states for psychosis and their clinical outcomes. *Br J Psychiatry*. 2009;195:218–26.
22. Mechelli A, Riecher-Rössler A, Meisenzahl EM, Tognin S, Wood SJ, Borgwardt SJ, et al. Neuroanatomical abnormalities that predate the onset of psychosis: a multicenter study. *Arch Gen Psychiatry*. 2011;68:489.
23. Satterthwaite TD, Wolf DH, Calkins ME, Vandekar SN, Erus G, Ruparel K, et al. Structural brain abnormalities in youth with psychosis spectrum symptoms. *JAMA Psychiatry*. 2016;73:515.
24. Wood SJ, Pantelis C, Velakoulis D, Yucel M, Fornito A, McGorry PD. Progressive changes in the development toward schizophrenia: studies in subjects at increased symptomatic risk. *Schizophr Bull*. 2007;34:322–9.
25. the Alzheimer's Disease Neuroimaging Initiative, EPiGEN Consortium, IMAGEN Consortium, Saguenay Youth Study (SYS) Group, Thompson PM, Stein JL, Medland SE, Hibar DP, Vasquez AA, et al. The ENIGMA Consortium: large-scale collaborative analyses of neuroimaging and genetic data. *Brain Imaging Behav*. 2014;8:153–82.
26. Andreou C, Borgwardt S. Structural and functional imaging markers for susceptibility to psychosis. *Mol Psychiatry*. 2020;25:2773–85.
27. de Wit S, Ziermans TB, Nieuwenhuis M, Schothorst PF, van Engeland H, Kahn RS, et al. Individual prediction of long-term outcome in adolescents at ultra-high risk for psychosis: Applying machine learning techniques to brain imaging data: Individual Outcome Prediction With MRI. *Hum Brain Mapp*. 2017;38:704–14.
28. Tognin S, Pettersson-Yeo W, Valli I, Hutton C, Woolley J, Allen P, et al. Using structural neuroimaging to make quantitative predictions of symptom progression in individuals at ultra-high risk for psychosis. *Front Psychiatry*. 2014;4:187.
29. Bzdok D, Meyer-Lindenberg A. Machine learning for precision psychiatry: opportunities and challenges. *Biol Psychiatry Cogn Neurosci Neuroimaging*. 2018;3:223–30.
30. Feczko E, Miranda-Dominguez O, Marr M, Graham AM, Nigg JT, Fair DA. The heterogeneity problem: approaches to identify psychiatric subtypes. *Trends Cogn Sci*. 2019;23:584–601.
31. Winkelbeiner S, Leucht S, Kane JM, Homan P. Evaluation of differences in individual treatment response in schizophrenia spectrum disorders: a meta-analysis. *JAMA Psychiatry*. 2019;76:1063.
32. Brugger SP, Howes OD. Heterogeneity and homogeneity of regional brain structure in schizophrenia: a meta-analysis. *JAMA Psychiatry*. 2017;74:1104.
33. Vissink CE, Winter-van Rossum I, Cannon TD, Fusar-Poli P, Kahn RS, Bossong MG. Structural brain volumes of individuals at clinical high risk for psychosis: a meta-analysis. *Biol Psychiatry Glob Open Sci*. 2022;2:147–52.
34. Doucet GE, Moser DA, Rodrigue A, Bassett DS, Glahn DC, Frangou S. Person-based brain morphometric similarity is heritable and correlates with biological features. *Cereb Cortex*. 2019;29:852–62.
35. Doucet GE, Glahn DC, Frangou S. Person-based similarity in brain structure and functional connectivity in bipolar disorder. *J Affect Disord*. 2020;276:38–44.
36. Doucet GE, Lin D, Du Y, Fu Z, Glahn DC, Calhoun VD, et al. Personalized estimates of morphometric similarity in bipolar disorder and schizophrenia. *Npj Schizophr*. 2020;6:39.
37. Antoniadis M, Haas SS, Modabbernia A, Bykowsky O, Frangou S, Borgwardt S, et al. Personalized estimates of brain structural variability in individuals with early psychosis. *Schizophr Bull*. 2021;47:1029–38.
38. Benchimol EI, Smeeth L, Guttmann A, Harron K, Moher D, Petersen I, et al. The REporting of Studies Conducted using Observational Routinely-collected health Data (RECORD) Statement. *PLoS Med*. 2015;12:e1001885.
39. Miller TJ, McGlashan TH, Woods SW, Stein K, Driesen N, Corcoran CM, et al. Symptom assessment in schizophrenic prodromal states. *Psychiatr Q*. 1999;70:273–87.
40. Miller TJ, McGlashan TH, Rosen JL, Cadenhead K, Ventura J, McFarlane W, et al. Prodromal assessment with the structured interview for prodromal syndromes and the scale of prodromal symptoms: predictive validity, interrater reliability, and training to reliability. *Schizophr Bull*. 2003;29:703–15.
41. Dale AM, Fischl B, Sereno MI. Cortical surface-based analysis. *Neuroimage*. 1999;9:179–94.
42. Fischl B, Sereno MI, Dale AM. Cortical surface-based analysis. *Neuroimage*. 1999;9:195–207.
43. Fischl B, Salat DH, Busa E, Albert M, Dieterich M, Haselgrove C, et al. Whole brain segmentation. *Neuron*. 2002;33:341–55.
44. Fischl B, Dale AM. Measuring the thickness of the human cerebral cortex from magnetic resonance images. *Proc Natl Acad Sci USA*. 2000;97:11050–5.
45. Collins DL, Neelin P, Peters TM, Evans AC. Automatic 3D intersubject registration of MR volumetric data in standardized Talairach space. *J Comput Assist Tomogr*. 1994;18:192–205.
46. Ségonne F, Dale AM, Busa E, Glessner M, Salat D, Hahn HK, et al. A hybrid approach to the skull stripping problem in MRI. *Neuroimage*. 2004;22:1060–75.
47. Fischl B, Salat DH, van der Kouwe AJW, Makris N, Ségonne F, Quinn BT, et al. Sequence-independent segmentation of magnetic resonance images. *Neuroimage*. 2004;23:569–84.
48. Sled JG, Zijdenbos AP, Evans AC. A nonparametric method for automatic correction of intensity nonuniformity in MRI data. *IEEE Trans Med Imaging*. 1998;17:87–97.
49. Desikan RS, Ségonne F, Fischl B, Quinn BT, Dickerson BC, Blacker D, et al. An automated labeling system for subdividing the human cerebral cortex on MRI scans into gyral based regions of interest. *Neuroimage*. 2006;31:968–80.
50. Radua J, Vieta E, Shinohara R, Kochunov P, Quidé Y, Green MJ, et al. Increased power by harmonizing structural MRI site differences with the ComBat batch adjustment method in ENIGMA. *Neuroimage*. 2020;218:116956.
51. Johnson WE, Li C, Rabinovic A. Adjusting batch effects in microarray expression data using empirical Bayes methods. *Biostatistics*. 2007;8:118–27.
52. for the ENIGMA Schizophrenia Working Group, van Erp TGM, Hibar DP, Rasmussen JM, Glahn DC, Pearson GD, et al. Subcortical brain volume abnormalities in 2028 individuals with schizophrenia and 2540 healthy controls via the ENIGMA consortium. *Mol Psychiatry*. 2016;21:547–53.
53. R Core Team. R: A language and environment for statistical computing. R Core Team [Internet]. Vienna: R Foundation for Statistical Computing; 2020.
54. Viechtbauer W. The Comprehensive R Archive Network. Package 'metafor'. 2015. <http://cran.r-project.org/web/packages/metafor/metafor.pdf>
55. Schwarzer G. The R Foundation for Statistical Computing 9. 2012. <https://mirror-hk.koddos.net/CRAN/web/packages/meta/meta.pdf>
56. Radua J, Davies C, Fusar-Poli P. Evaluation of variability in individual response to treatments in the clinical high-risk state for psychosis: a meta-analysis. *Schizophr Res*. 2021;227:20–7.
57. Benjamini Y, Hochberg Y. Controlling the false discovery rate: a practical and powerful approach to multiple testing. *J R Stat Soc Ser B Methodol*. 1995;57:289–300.
58. Ding Y, Ou Y, Pan P, Shan X, Chen J, Liu F, et al. Brain structural abnormalities as potential markers for detecting individuals with ultra-high risk for psychosis: a systematic review and meta-analysis. *Schizophr Res*. 2019;209:22–31.
59. Fusar-Poli P, Borgwardt S, Crescini A, Deste G, Kempton MJ, Lawrie S, et al. Neuroanatomy of vulnerability to psychosis: a voxel-based meta-analysis. *Neurosci Biobehav Rev*. 2011;35:1175–85.
60. Fusar-Poli P, Broome MR, Woolley JB, Johns LC, Tabraham P, Bramon E, et al. Altered brain function directly related to structural abnormalities in people at ultra high risk of psychosis: longitudinal VBM-fMRI study. *J Psychiatr Res*. 2011;45:190–8.
61. Catalan A, Salazar de Pablo G, Aymerich C, Damiani S, Sordi V, Radua J, et al. Neurocognitive functioning in individuals at clinical high-risk for psychosis: systematic review and meta-analysis. *JAMA Psychiatry*. 2021. <https://doi.org/10.1001/jamapsychiatry.2021.1290>.
62. Pantelis C, Velakoulis D, McGorry PD, Wood SJ, Suckling J, Phillips LJ, et al. Neuroanatomical abnormalities before and after onset of psychosis: a cross-sectional and longitudinal MRI comparison. *Lancet* 2003;361:281–8.
63. Harrisberger F, Buechler R, Smieskova R, Lenz C, Walter A, Egloff L, et al. Alterations in the hippocampus and thalamus in individuals at high risk for psychosis. *Npj Schizophr*. 2016;2:16033.
64. Provenzano FA, Guo J, Wall MM, Feng X, Sigmon HC, Brucato G, et al. Hippocampal pathology in clinical high-risk patients and the onset of schizophrenia. *Biol Psychiatry*. 2020;87:234–42.
65. Walter A, Studerus E, Smieskova R, Kuster P, Aston J, Lang UE, et al. Hippocampal volume in subjects at high risk of psychosis: a longitudinal MRI study. *Schizophr Res*. 2012;142:217–22.
66. Wood SJ, Kennedy D, Phillips LJ, Seal ML, Yücel M, Nelson B, et al. Hippocampal pathology in individuals at ultra-high risk for psychosis: a multi-modal magnetic resonance study. *Neuroimage*. 2010;52:62–8.
67. Marquand AF, Rezek I, Buitelaar J, Beckmann CF. Understanding heterogeneity in clinical cohorts using normative models: beyond case-control studies. *Biol Psychiatry*. 2016;80:552–61.
68. Addington J, Cornblatt BA, Cadenhead KS, Cannon TD, McGlashan TH, Perkins DO, et al. At clinical high risk for psychosis: outcome for nonconverters. *Am J Psychiatry*. 2011;168:800–5.
69. Carrión RE, Auther AM, McLaughlin D, Addington J, Bearden CE, Cadenhead KS, et al. Social decline in the psychosis prodrome: predictor potential and heterogeneity of outcome. *Schizophr Res*. 2021;227:44–51.

70. Woods SW, Walsh BC, Addington J, Cadenhead KS, Cannon TD, Cornblatt BA, et al. Current status specifiers for patients at clinical high risk for psychosis. *Schizophr Res.* 2014;158:69–75.
71. Bae S. Is variance ratio a valid indicator of heterogeneous treatment effect? *JAMA Psychiatry.* 2020;77:216.
72. Rapp C, Bugra H, Riecher-Rössler A, Tamagni C, Borgwardt S. Effects of cannabis use on human brain structure in psychosis: a systematic review combining in vivo structural neuroimaging and post mortem studies. *Curr Pharm Des.* 2012;18:5070–80.
73. Stone JM, Bhattacharyya S, Barker GJ, McGuire PK. Substance use and regional gray matter volume in individuals at high risk of psychosis. *Eur Neuropsychopharmacol.* 2012;22:114–22.
74. Addington J, Farris M, Devoue D, Metzrak P. Progression from being at-risk to psychosis: next steps. *npj Schizophr.* 2020;6:27.
75. Jonas KG, Lencz T, Li K, Malhotra AK, Perlman G, Fochtmann LJ, et al. Schizophrenia polygenic risk score and 20-year course of illness in psychotic disorders. *Transl Psychiatry.* 2019;9:300.

AUTHOR CONTRIBUTIONS

Database management of the ENIGMA CHR Working Group data set is conducted by MJ, DH and PMT. Data analysis was conducted by HB with significant input from JR, MA, SSH, SF, MJ, DH and PFP. The first draft of the manuscript was compiled by HB with significant input and critical review from all authors (JR, MA, SSH, SF, IA, PA, OAA, KA, PB, IB, CFB, MWLC, TC, RC, CMC, VLC, BHE, AF, LBG, HKH, KMH, RAH, YH, KH, MK, KK, NK, MK, JK, MLK, SK, AK, TDK, YBK, JSK, SML, IL, JL, AL, RLL, DHM, CM, RM, PM, BN, TN, DN, MAO, CP, JMR, JIR, WR, DFS, DS, US, LS, GS, MS, TT, CKT, JT, AT, SIT, AST, PUJ, TGV, TAMJV, TGMV, JAW, LTW, SJW, JHZ, PM, PMT, MJ, DH, PFP). All ENIGMA CHR Working Group members offered substantial contributions to either the collection or processing of local data.

FUNDING

HB is funded by a National Institute for Health Research (NIHR) Maudsley Biomedical Research Centre doctoral studentship. SF is supported by the National Institute of Mental Health under grant R01MH113619. CMC is supported by R01MH107558 and R01MH115332. BN is supported by a National Health and Medical Research Council (NHMRC) Senior Research Fellowship (1137687). AL is supported by a National Health and Medical Research Council (NHMRC) Senior Research Fellowship (#1148793). CKT is supported by the Research Council of Norway (223273, 288083, 323951) and the South-Eastern Norway Regional Health Authority (2019069, 2021070, 500189). PMT is supported by NIH grants R01MH116147, P41EB015922, and R01AG058854. VC is supported by a National Health and Medical Research Council (NHMRC) Investigator Grant (1177370). LTW is supported by the European Research Council under the European Union's Horizon 2020 research and Innovation program (ERC StG, Grant 802998). GS is supported by the Fundació Clínic Recerca Biomèdica, the Brain and Behavior Research Foundation (NARSAD Young Investigator Award 2017, grant ID: 26731), the Alicia Koplowitz Foundation and the Spanish Ministry of Health, Instituto

de Salud Carlos III "Health Research Fund" (PI15/0444; PI18/0242; PI18/00976). CF-S was supported by grants 182279 and 261895 from the Consejo Nacional de Ciencia y Tecnología, grants from CONACYT's Sistema Nacional de Investigadores, and grant R21 MH117434 from the National Institutes of Health. CP was supported by a National Health and Medical Research Council (NHMRC) Senior Principal Research Fellowship (1105825), an NHMRC L3 Investigator Grant (1196508), and NHMRC Program Grant (ID: 1150083). Core funding for ENIGMA was provided by the NIH Big Data to Knowledge (BD2K) program under consortium grant U54 EB020403 to PMT.

COMPETING INTERESTS

PMT receives partial research support from Biogen, Inc., for research unrelated to this manuscript. OAA is a consultant to HealthLytx. CP has received honoraria for talks at educational meetings and has served on an advisory board for Lundbeck, Australia Pty Ltd. BHE has received lecture fees Otsuka Pharma Scandinavia AB, Boehringer Ingelheim, and Lundbeck Pharma A/S.

ADDITIONAL INFORMATION

Supplementary information The online version contains supplementary material available at <https://doi.org/10.1038/s41398-022-02057-y>.

Correspondence and requests for materials should be addressed to Helen Baldwin.

Reprints and permission information is available at <http://www.nature.com/reprints>

Publisher's note Springer Nature remains neutral with regard to jurisdictional claims in published maps and institutional affiliations.



Open Access This article is licensed under a Creative Commons Attribution 4.0 International License, which permits use, sharing, adaptation, distribution and reproduction in any medium or format, as long as you give appropriate credit to the original author(s) and the source, provide a link to the Creative Commons license, and indicate if changes were made. The images or other third party material in this article are included in the article's Creative Commons license, unless indicated otherwise in a credit line to the material. If material is not included in the article's Creative Commons license and your intended use is not permitted by statutory regulation or exceeds the permitted use, you will need to obtain permission directly from the copyright holder. To view a copy of this license, visit <http://creativecommons.org/licenses/by/4.0/>.

© The Author(s) 2022

Helen Baldwin ^{1,2,✉}, Joaquim Radua^{1,3,4}, Mathilde Antoniades⁵, Shalaila S. Haas ⁵, Sophia Frangou^{5,6}, Ingrid Agartz^{7,8,9,10}, Paul Allen^{11,12}, Ole A. Andreassen ^{10,13}, Kimberley Atkinson¹⁴, Peter Bachman¹⁵, Inmaculada Baeza¹⁶, Cali F. Bartholomeusz^{17,18}, Michael W. L. Chee ¹⁹, Tiziano Colibazzi^{20,21}, Rebecca E. Cooper²², Cheryl M. Corcoran ^{5,23}, Vanessa L. Cropley ^{22,24}, Bjørn H. Ebdrup ^{25,26}, Adriana Fortea²⁷, Louise Birkedal Glenthøj²⁸, Holly K. Hamilton^{29,30}, Kristen M. Haut³¹, Rebecca A. Hayes¹⁵, Ying He³², Karsten Heekeren ^{33,34}, Michael Kaess^{35,36}, Kiyoto Kasai ^{37,38,39}, Naoyuki Katagiri⁴⁰, Minah Kim ^{41,42}, Jochen Kindler³⁶, Mallory J. Klaunig⁴³, Shinsuke Koike ^{38,44}, Alex Koppel⁴⁵, Tina D. Kristensen ^{25,28}, Yoo Bin Kwak^{46,47}, Jun Soo Kwon ^{41,42}, Stephen M. Lawrie ¹⁴, Irina Lebedeva⁴⁸, Jimmy Lee ^{47,49}, Ashleigh Lin⁵⁰, Rachel L. Loewy²⁹, Daniel H. Mathalon ^{29,30}, Chantal Michel³⁶, Romina Mizrahi ^{51,52}, Paul Møller⁵³, Barnaby Nelson ⁴⁰, Takahiro Nemoto ²⁸, Dorte Nordholm²⁸, Maria A. Omelchenko⁵⁴, Christos Pantelis ^{22,55}, Jayachandra M. Raghava^{25,56,57}, Jan I. Rössberg¹³, Wulf Rössler^{34,58}, Dean F. Salisbury¹⁵, Daiki Sasabayashi ^{59,60}, Ulrich Schall^{61,62}, Lukasz Smigielski ^{34,63}, Gisela Sugranyes ¹⁶, Michio Suzuki^{59,60}, Tsutomu Takahashi ^{59,60}, Christian K. Tamnes ^{7,13,64}, Jinsong Tang^{65,66}, Anastasia Theodoridou ³⁴, Sophia I. Thomopoulos⁶⁷, Alexander S. Tomyshev⁴⁸, Peter J. Uhlhaas^{68,69}, Tor G. Værnes^{13,70}, Therese A. M. J. van Amelsvoort⁷¹, Theo G. M. Van Erp ^{72,73}, James A. Waltz ⁷⁴, Lars T. Westlye ^{10,13,75}, Stephen J. Wood^{17,18,76}, Juan H. Zhou ^{19,77}, Philip McGuire ¹², Paul M. Thompson⁶⁷, Maria Jalbrzikowski^{15,78,79}, Dennis Hernaus⁷¹, Paolo Fusar-Poli^{1,2,80,81} and the ENIGMA Clinical High Risk for Psychosis Working Group

¹Early Psychosis: Interventions and Clinical-detection (EPIC) Lab, Department of Psychosis Studies, Institute of Psychiatry, Psychology & Neuroscience, King's College London, London, UK. ²National Institute for Health Research, Maudsley Biomedical Research Centre, South London and Maudsley NHS Foundation Trust, London, UK. ³Institut d'Investigacions Biomèdiques August Pi i Sunyer, CIBERSAM, Barcelona, Spain. ⁴Department of Clinical Neuroscience, Karolinska Institutet, Stockholm, Sweden. ⁵Department of Psychiatry, Icahn School of Medicine at Mount Sinai, New York City, NY, USA. ⁶Department of Psychiatry, University of British Columbia, Vancouver, BC, Canada. ⁷Department of Psychiatric Research, Diakonhjemmet Hospital, Oslo, Norway. ⁸Centre for Psychiatry Research, Department of Clinical Neuroscience, Karolinska Institutet & Stockholm Health Care

Services, Stockholm County Council, Stockholm, Sweden. ⁹Norwegian Centre for Mental Disorders Research, Institute of Clinical Medicine, University of Oslo, Oslo, Norway. ¹⁰KG Jebsen Center for Neurodevelopmental Disorders, University of Oslo, Oslo, Norway. ¹¹Department of Psychology, University of Roehampton, London, UK. ¹²Department of Psychosis Studies, Institute of Psychiatry, Psychology and Neuroscience, King's College London, London, UK. ¹³NORMENT, Division of Mental Health and Addiction, Oslo University Hospital & Institute of Clinical Medicine, University of Oslo, Oslo, Norway. ¹⁴Division of Psychiatry, University of Edinburgh, Edinburgh, UK. ¹⁵Department of Psychiatry, University of Pittsburgh, Pittsburgh, PA, USA. ¹⁶Department of Child and Adolescent Psychiatry and Psychology, Institute of Neuroscience, 20175GR-881, Hospital Clinic Barcelona, Institut d'Investigacions Biomèdiques August Pi i Sunyer (IDIBAPS), Centro de Investigación Biomédica en Red de Salud Mental (CIBERSAM), Universitat de Barcelona, Barcelona, Spain. ¹⁷Centre for Youth Mental Health, University of Melbourne, Melbourne, VIC, Australia. ¹⁸Orygen, Melbourne, VIC, Australia. ¹⁹Center for Sleep and Cognition, Yong Loo Lin School of Medicine, National University of Singapore, Singapore, Singapore. ²⁰Department of Psychiatry, Columbia University, New York City, NY, USA. ²¹New York State Psychiatric Institute, New York City, NY, USA. ²²Melbourne Neuropsychiatry Centre, Department of Psychiatry, University of Melbourne & Melbourne Health, Carlton South, VIC, Australia. ²³Mental Illness Research, Education, and Clinical Center, James J Peters VA Medical Center, New York City, NY, USA. ²⁴Centre for Mental Health, Faculty of Health, Arts and Design, School of Health Sciences, Swinburne University, Melbourne, VIC, Australia. ²⁵Centre for Neuropsychiatric Schizophrenia Research (CNSR), Mental Health Centre Glostrup, Copenhagen University Hospital, Glostrup, Denmark. ²⁶Department of Clinical Medicine, Faculty of Health and Medical Sciences, University of Copenhagen, Copenhagen, Denmark. ²⁷Department of Child and Adolescent Psychiatry and Psychology, Institute of Neuroscience, Hospital Clinic Barcelona, Fundació Clínic Recerca Biomèdica, Universitat de Barcelona, Barcelona, Spain. ²⁸Copenhagen Research Center for Mental Health, Mental Health Center Copenhagen, University of Copenhagen, Copenhagen, Denmark. ²⁹Department of Psychiatry and Behavioral Sciences, University of California San Francisco, San Francisco, CA, USA. ³⁰San Francisco Veterans Affairs Health Care System, San Francisco, CA, USA. ³¹Department of Psychiatry and Behavioral Sciences, Rush University Medical Center, Chicago, IL, USA. ³²National Clinical Research Center for Mental Disorders and Department of Psychiatry, The Second Xiangya Hospital of Central South University, Changsha, Hunan, China. ³³Department of Psychiatry and Psychotherapy I, LVR-Hospital Cologne, Cologne, Germany. ³⁴Department of Psychiatry, Psychotherapy and Psychosomatics, Psychiatric University Hospital Zurich, University of Zurich, Zurich, Switzerland. ³⁵Department of Child and Adolescent Psychiatry, Center of Psychosocial Medicine, University of Heidelberg, Heidelberg, Germany. ³⁶University Hospital of Child and Adolescent Psychiatry and Psychotherapy, University of Bern, Bern, Switzerland. ³⁷Department of Neuropsychiatry, Graduate School of Medicine, The University of Tokyo, Tokyo, Japan. ³⁸The University of Tokyo Institute for Diversity and Adaptation of Human Mind, Tokyo, Japan. ³⁹The International Research Center for Neurointelligence at The University of Tokyo Institutes for Advanced Study, The University of Tokyo, Tokyo, Japan. ⁴⁰Department of Neuropsychiatry, Toho University School of Medicine, Tokyo, Japan. ⁴¹Department of Neuropsychiatry, Seoul National University Hospital, Seoul, Republic of Korea. ⁴²Department of Psychiatry, Seoul National University College of Medicine, Seoul, Republic of Korea. ⁴³Department of Psychology, University of Maryland, Baltimore County, MD, USA. ⁴⁴Center for Evolutionary Cognitive Sciences, Graduate School of Art and Sciences, The University of Tokyo, Tokyo, Japan. ⁴⁵Department of Pharmacology and Toxicology, University of Toronto, Toronto, ON, Canada. ⁴⁶Department of Brain and Cognitive Sciences, Seoul National University College of Natural Sciences, Seoul, Republic of Korea. ⁴⁷Department of Psychosis, Institute of Mental Health, Singapore, Singapore. ⁴⁸Laboratory of Neuroimaging and Multimodal Analysis, Mental Health Research Center, Moscow, Russian Federation. ⁴⁹Lee Kong Chian School of Medicine, Nanyang Technological University, Singapore, Singapore. ⁵⁰Telethon Kids Institute, The University of Western Australia, Perth, WA, Australia. ⁵¹Douglas Research Center, Montreal, QC, Canada. ⁵²Department of Psychiatry, McGill University, Montreal, QC, Canada. ⁵³Department for Mental Health Research and Development, Division of Mental Health and Addiction, Vestre Viken Hospital Trust, Drammen, Norway. ⁵⁴Department of Youth Psychiatry, Mental Health Research Center, Moscow, Russian Federation. ⁵⁵Florey Institute of Neuroscience and Mental Health, Center for Mental Health, Parkville, VIC, Australia. ⁵⁶Department of Clinical Physiology, Nuclear Medicine and PET, Functional Imaging Unit, University of Copenhagen, Glostrup, Denmark. ⁵⁷Centre for Neuropsychiatric Schizophrenia Research, Mental Health Centre Glostrup, University of Copenhagen, Glostrup, Denmark. ⁵⁸Department of Psychiatry and Psychotherapy, Charité Universitätsmedizin Berlin, Berlin, Germany. ⁵⁹Department of Neuropsychiatry, University of Toyama Graduate School of Medicine and Pharmaceutical Sciences, Toyama, Japan. ⁶⁰Research Center for Idling Brain Science, University of Toyama, Toyama, Japan. ⁶¹Priority Centre for Brain and Mental Health Research, The University of Newcastle, Newcastle, NSW, Australia. ⁶²Priority Research Centre Grow Up Well, The University of Newcastle, Newcastle, NSW, Australia. ⁶³Department of Child and Adolescent Psychiatry, Psychiatric University Zurich, University of Zurich, Zurich, Switzerland. ⁶⁴PROMENTA Research Center, Department of Psychology, University of Oslo, Oslo, Norway. ⁶⁵Department of Psychiatry, Sir Run Run Shaw Hospital, School of Medicine, Zhejiang University, Hangzhou, China. ⁶⁶Key Laboratory of Medical Neurobiology of Zhejiang Province, School of Medicine, Zhejiang University, Hangzhou, China. ⁶⁷Imaging Genetics Center, Mark and Mary Stevens Neuroimaging and Informatics Institute, Keck School of Medicine, University of Southern California, Los Angeles, CA, USA. ⁶⁸Institute of Neuroscience and Psychology, University of Glasgow, Glasgow, UK. ⁶⁹Department of Child and Adolescent Psychiatry, Charité Universitätsmedizin, Berlin, Germany. ⁷⁰Early Intervention in Psychosis Advisory Unit for South-East Norway, TIPS Sør-Øst, Division of Mental Health and Addiction, Oslo University Hospital, Oslo, Norway. ⁷¹Department of Psychiatry and Neuropsychology, School for Mental Health and Neuroscience, Faculty of Health Medicine and Life Sciences, Maastricht University, Maastricht, The Netherlands. ⁷²Center for the Neurobiology of Learning and Memory, University of California Irvine, Irvine, CA, USA. ⁷³Clinical Translational Neuroscience Laboratory, Department of Psychiatry and Human Behavior, University of California Irvine, Irvine, CA, USA. ⁷⁴Maryland Psychiatric Research Center, University of Maryland School of Medicine, Baltimore, MD, USA. ⁷⁵Department of Psychology, University of Oslo, Oslo, Norway. ⁷⁶School of Psychology, University of Birmingham, Birmingham, UK. ⁷⁷Center for Translational Magnetic Resonance Research, Yong Loo Lin School of Medicine, National University of Singapore, Singapore, Singapore. ⁷⁸Department of Psychiatry and Behavioral Sciences, Boston Children's Hospital, Boston, MA, USA. ⁷⁹Department of Psychiatry, Harvard Medical School, Cambridge, MA, USA. ⁸⁰OASIS Service, South London and Maudsley NHS Foundation Trust, London, UK. ⁸¹Department of Brain and Behavioural Sciences, University of Pavia, Pavia, Italy. ⁸²email: helen.baldwin@kcl.ac.uk

THE ENIGMA CLINICAL HIGH RISK FOR PSYCHOSIS WORKING GROUP

Camilo de la Fuente-Sandoval⁸², Sabrina Catalano¹⁵, Daniela Hubl⁸³, Jason Schiffman^{43,84}, Enea D. Venegoni^{14,71}, Christine I. Hooker³¹, Paul E. Rasser^{61,85}, Wenche ten Velden Hegelstad^{86,87}, Franz Resch⁸⁸, Imke L. J. Lemmers-Jansen^{12,89}, G. Paul Amminger^{17,18}, Xiaogang Chen^{32,90}, Kang Ik K. Cho⁹¹, Birte Yding Glenthøj^{25,26}, Lieuwe de Haan^{92,93}, Matthew A. Harris¹⁴, Wu Jeong Hwang⁴⁶, Pablo León-Ortiz⁸², Xiaoqian Ma³², Patrick McGorry^{17,18}, Ricardo Mora-Durán^{82,94}, Masafumi Mizuno⁹⁵, Merete Nordentoft²⁸, Lijun Ouyang^{32,90,96}, Jose C. Pariente⁹⁷, Francisco Reyes-Madriral⁸², Mikkel E. Sørensen²⁵, Dennis Velakoulis^{22,98}, Sophia Vinogradov⁹⁹, Christina Wenneberg²⁸, Hidenori Yamasue¹⁰⁰, Liu Yuan^{32,90,96} and Alison R. Yung^{17,18}

⁸²Laboratory of Experimental Psychiatry, Instituto Nacional de Neurología y Neurocirugía, Mexico City, Mexico. ⁸³Translational Research Center, University Hospital of Psychiatry and Psychotherapy, University of Bern, Bern, Switzerland. ⁸⁴Department of Psychological Science, University of California Irvine, Irvine, CA, USA. ⁸⁵Priority Research Centre for Stroke and Brain Injury, The University of Newcastle, Newcastle, NSW, Australia. ⁸⁶Faculty of Social Sciences, University of Stavanger, Stavanger, Norway. ⁸⁷TIPS Centre for Clinical Research in Psychosis, Stavanger University Hospital, Stavanger, Norway. ⁸⁸Clinic for Child and Adolescent Psychiatry, University Hospital of Heidelberg, Heidelberg, Germany. ⁸⁹Faculty of Behavioural and Movement Sciences, Department of Clinical, Neuro and Developmental Psychology, Vrije Universiteit Amsterdam, Amsterdam, the Netherlands. ⁹⁰National Clinical Research Center for Geriatric Disorders, Xiangya Hospital, Central South University, Changsha, Hunan, China. ⁹¹Department of Psychiatry, Psychiatry Neuroimaging Laboratory, Brigham and Women's Hospital, Harvard Medical School, Boston, MA, USA. ⁹²Department of Psychiatry, Amsterdam University Medical Centre, Amsterdam, the Netherlands. ⁹³Arkin, Amsterdam, the Netherlands. ⁹⁴Emergency Department, Hospital Fray Bernardino Álvarez, Mexico City, Mexico. ⁹⁵Tokyo Metropolitan Matsuzawa Hospital, Tokyo, Japan. ⁹⁶Hunan Key Laboratory of Psychiatry and Mental Health, the Second Xiangya Hospital, Central South University, Changsha, Hunan, China. ⁹⁷Magnetic Resonance Imaging Core Facility, Institut d'Investigacions Biomèdiques August Pi i Sunyer, Barcelona, Spain. ⁹⁸Neuropsychiatry, The Royal Melbourne Hospital, Melbourne, VIC, Australia. ⁹⁹Department of Psychiatry & Behavioral Sciences, University of Minnesota, Minneapolis, MN, USA. ¹⁰⁰Department of Psychiatry, Hamamatsu University School of Medicine, Hamamatsu, Japan.